ELSEVIER

Journal of Molecular Structure 643 (2002) 55–68

Journal of
MOLECULAR
STRUCTURE

www.elsevier.com/locate/molstruc

# Deprotonation of *N*-phenacyl- and *N*-acetonyl-4-cyanopyridinium halides with 1,4-diazabicyclo[2,2,2]octane

M. Szafran*, A. Szwajca, B. Łęska, G. Schroeder, Z. Dega-Szafran

*Faculty of Chemistry, Adam Mickiewicz University, ul Grunwaldzka 6, 60780 Poznań, Poland*

Received 12 March 2002; revised 27 June 2002; accepted 12 July 2002

## Abstract

In *N*-phenacyl- and *N*-acetonyl-4-cyanopyridinium halides (**1a·Br** and **1b·Cl**) the $N^+CH_2$ hydrogens are replaced by deuterium in $D_2O$ or $CH_3OD$ solutions, similarly as in β-diketones, proving a prototropic equilibrium **1** $\rightleftharpoons$ **2**. The rate constants have been measured for deprotonation of **1a·Br** and **1b·Cl** with 1,4-diazabicyclo[2,2,2]octane (DABCO) in solutions. UV, FTIR, $^1$H and $^{13}$C NMR spectra are consistent with the ylide structure of the deprotonated species. *N*-phenacyl-4-cyanopyridinium ylide (**3a**) is relatively stable in the solid state and unstable in solutions. The observed parallel changes in $\Delta S^{\neq}$ and the time of disappearance of the ylide absorption band suggest that solvation is responsible for the ylide stability. The UV–Vis spectra of **1a·Br** and **1b·Cl** with DABCO show solvent dependent isosbestic points, which suggest that the decomposition reactions of ylides are very probably uniform. The PM3 and B3LYP calculations were carried out to investigate the structures of the cations, ylides and their complexes with ammonia and DABCO. Ylides are formed by abstraction of hydroxy proton from enol form (**2**) via complex **8**.

*Keywords:* *N*-phenacyl-4-cyanopyridinium bromide; *N*-acetonyl-4-cyanopyridinium chloride; Deprotonation reaction; Ylides; Spectroscopy; DFT and PM3 calculations

## 1. Introductions

In *N*-alkyl-pyridinium salts of the type $\geq N^+-CH_2-Y$, where Y is a strong electron-withdrawing substituent, the methylene protons are acidic and their reactivity becomes comparable with that of methylene group of 1,3-dicarbonyl compounds. The p$K_a$ values of a number of *N*-phenacyl-pyridinium salts are in the 7–10.9 range [1,2], acetylacetone 8.16 and benzoylacetone 8.23 [3]. In crystals, 1,3-diketones exist in enolate form, connected by intramolecular or intermolecular O–H···O hydrogen bonds with O···O distance in the 2.465–2.629 Å range [4]. 1,3-Dicarbonyl compounds in solutions may exist in three forms: the diketo, *cis*-enolic and *trans*-enolic [5]. The equilibrium constants of acetyloacetone, $K_T = [cis\text{-enolic}]/[\text{diketo}]$ are solvent dependent and change from 19 in hexane to 1.6 in DMSO [6]. *N*-phenacyl-pyridinium ion in aqueous solution exists mainly in the keto form (**1**) with some amount of the enol form (**2**) (Schemes 1 and 2); $K_T = [\text{enol }(\mathbf{2})]/[\text{keto}(\mathbf{1})] = 7.7 \times 10^{-7}$ [2].

In basic solutions the *N*-phenacyl-pyridinium ion rapidly generates an ylide, which also can exists in an

---

* Corresponding author. Tel.: +48-61-829-13209; fax: +48-61-865-8008.

*E-mail address:* szafran@main.amu.edu.pl (M. Szafran).

0022-2860/02/$ - see front matter © 2002 Elsevier Science B.V. All rights reserved.
PII: S0022-2860(02)00394-0

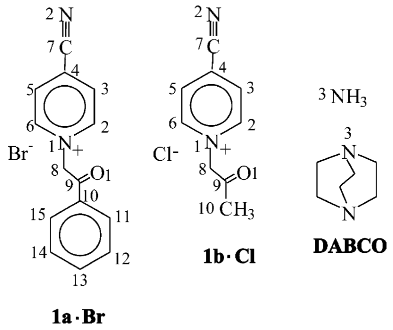

Scheme 1.

equilibrium between zwitterion (**3**) and betaine (**4**). Although nitrogen ylides are widely used as intermediate in organic synthesis [7–10], no systematic study of their formation rate has been reported. We have recently presented [11] a detailed kinetic study of the deprotonation reaction of several quaternary pyridinium halides, $(4\text{-R–C}_5H_4N^+CH_2Y)X^-$; R = Me and $NMe_2$, Y = $CONH_2$, COOEt, COMe, $COC_6H_5$ and CN, X = Cl or Br, with very strong bases in DMSO solution. Now, we report on the deprotonation of more acidic *N*-phenacyl-4-cyanopyridinium bromide (**1a·Br**) and *N*-acetonyl-4-cyanopyridinium chloride (**1b·Cl**), which occurs with involvement of a much weaker base, such as 1,4-diazabicyclo[2,2,2]octane (DABCO) (Scheme 1).

## 2. Experimental

*N*-phenacyl-4-cyanopyridinium bromide (**1a·Br**) was prepared by refluxing of 4-cyanopyridine with the equimolar amount of $BrCH_2COPh$ in acetone for 10 h. The excess of the solvent was removed under reduced pressure, the crude product was washed with diethyl ether and recrystallized from methanol containing 2% HBr, mp 223–5 °C dec., 85% yield, Ref. [1] 236–7 °C dec.

*N*-acetonyl-4-cyanopyridinium chloride (**1b·Cl**) was prepared by refluxing of 4-cyanopyridine with the 10% excess of $ClCH_2COCH_3$ in acetonitrile for 10 h. The solvent was removed under reduced pressure, the crude product was washed with diethyl ether and recrystallized from ethanol containing 2% HCl, mp 205 °C dec., 43% yield.

*N*-phenacyl-4-cyanopyridinium ylide (**3a**) was obtained by mixing an aqueous solution of **1a·Br** and an aqueous solution of 20% sodium carbonate. The ylide was then filtered off and dried over $P_2O_5$, mp 126 °C dec., Ref. [1] 114–6 °C dec. *N*-acetonyl-4-cyanopyridinium ylide (**3b**) is soluble in water.

The NMR spectra were recorded on a Varian Gemini 300VT spectrometer, operating at 300.07 and 75.46 MHz for $^1$H and $^{13}$C, respectively. The FTIR spectra were recorded in Nujol and Fluorolube mulls on a Nicolet Magna spectrometer at 2 $cm^{-1}$ resolution. Each spectrum consists of 200 scans. The UV spectra were recorded on a JASCO V-550 spectrometer.

The rate of proton transfer was measured spectrophotometrically on an Applied Photophysics stopped-flow apparatus with the cell block thermostated to ± 1 °C. The reactions were monitored at the maximum absorption of ylide (**3a**, 468–496 nm and **3b**, 496 nm) and were conducted by mixing a solution of **1a·Br** ($1 \times 10^{-5}$ M) with 1,4-diazabicyclo[2,2,2]octane ($1–5 \times 10^{-4}$ M) in the following solvents: $H_2O$, MeOH, MeCN + 5% MeOH and DMSO, and **1b·Cl** ($1 \times 10^{-5}$ M) in $H_2O$.

The PM3 [12] semiempirical method was used, as implemented in the AMPAC program package [13]. In all cases, the PRECISE and GRAD key words were used. The DFT calculations have been carried out using the GAUSSIAN 98 package [14]. The calculations employed the BLYP and B3LYP functionals (Becke three-parameter Lee–Yang–Parr) exchange-correlation functional [15,16], which combines the hybrid exchange functional of Becke [15] with the gradient-corrected correlation functional of Lee, Yang and Parr [16].

## 3. Results and discussion

The $N^+CH_2$ hydrogens in **1a·Br** and **1b·Cl** are easily replaced by deuterium in $D_2O$ or $CH_3OD$ solutions. In a similar way the $CH_2$ hydrogens in acetylacetone were exchanged by deuterium in $D_2O$ solution [17]. On the other hand, in betaines, $\geq N^+CH_2COO^-$ and their hydrogen halides, $\geq N^+CH_2COOH{\cdot}X^-$, the $CH_2$ hydrogens are not replaced by deuterium in $D_2O$ solutions [18-20]. This confirms the presence of **2** in solutions of **1a·Br** and **1b·Cl**, which undergo

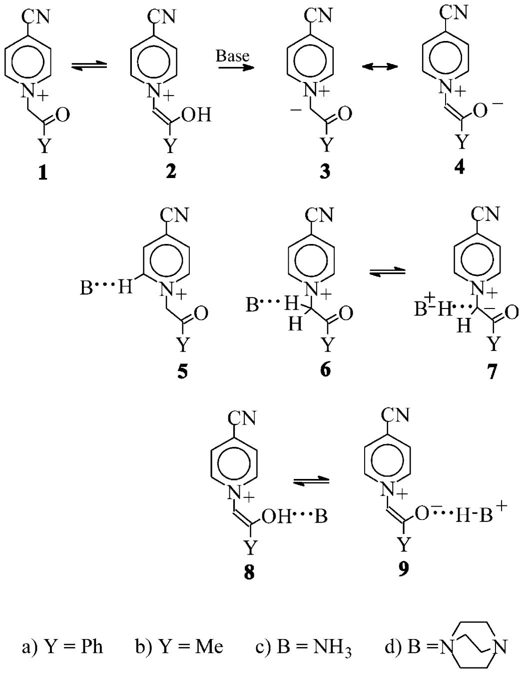

Scheme 2.

deprotonation on addition of 1,4-diazabicyclo[2,2,2]octane, DABCO ($pK_{BH} = 8.82$ [21], PA = 963.4 kJ $mol^{-1}$ [22]) to give **3a** and **3b** ylides, respectively (Scheme 2). The characteristic ylide absorption is solvent dependent (see below).

### 3.1. FTIR, UV–Vis and NMR spectra

In Fig. 1 the IR spectra of **1b·Cl** and **1a·Br** and their deuterated derivatives are compared. The $\nu CD_2$ vibrations are at 2216 and 2243 $cm^{-1}$, respectively. The $\nu$C=O band in **1a·Br** is at 1688 $cm^{-1}$, while in **3a** is at a fairly low frequency, 1522 $cm^{-1}$. Matsubayashi [23] explains this low frequency of the $\nu$C=O band by elongation of the C–O bond in ylides. The $C_9$–$O_1$ distances confirm this explanation (see below). In **1b·Cl** the $\nu$C=O band, as expected, is at a slightly higher frequency (1731 $cm^{-1}$).

The UV–Vis spectra of **1a·Br** (322 and 395 nm) and **1b·Cl** (269 and ~331 nm) with DABCO show two isosbestic points (Fig. 2), which suggest that the decomposition reactions of ylides are very probably uniform [24]. The isosbestic points are solvent dependent and in the case of **1a·Br** they are: 325 and 400 nm in $CHCl_3$, 242 nm in MeOH and 240 nm in $H_2O$. This suggests two different mechanisms of the decomposition reaction. In $CHCl_3$ ylide, **3a** decomposes to 4-cyanopyridine and phenacylo carbene, with a probable rearrangement to ketene or dimerized to 1,2-dibenzoylethylene. Formation of 4-cyanopyridine (α-H, 8.82, β-H, 7.54 ppm) was confirmed by $^1$H NMR spectroscopy (Fig. 3). From aqueous solution benzoic acid was separated. This indicates that in aqueous solution of ylides, the bond between $N^+$–CH and carbonyl groups is broken.

The $^1$H and $^{13}$C NMR chemical shifts of **1a·Br**, **1b·Cl**, **3a** and **3b** in DMSO-$d_6$ are listed in Table 1. The proton and carbon-13 signals have been easily assigned by comparison with the spectra of *N*-phenacyl-pyridinium halides [1,11,25], *N*-methyl-pyridinium iodide [26] and acetophenone [27]. The signal of α-protons of the pyridine ring in the ylide is broad and shifted downfield as compared to that of the α-protons of the pyridine ring in the starting salts. This broadening and deshielding can be explained by the interaction of these protons with the oxygen atom in the betaine form (**4**). Henrick et al. [28] have noted a similar NMR effect but attributed it to a deshielding of the α-protons resulting from the resonance structure.

### 3.2. Kinetic study of proton transfer to amine

When quaternary pyridinium halides (AH) are treated by an excess of a strong base (B) $\{[B_o] \gg [AH_o]\}$ the deprotonation reaction is described by Eq. (1) [29]:

$$A^+H + B \underset{k_-}{\overset{k}{\rightleftharpoons}} (A^\pm \cdots H{-}B^+) \overset{K_D}{\rightleftharpoons} A^\pm + B^+H; \qquad (1)$$

$$k_{obs} = k[B_0] + k_-[B^+H]/K_D$$

where $k$ is the rate constant for the deprotonation (forward) reaction, $k_-$ is the rate constant for the protonation (backward) reaction, $[B_0]$ is the initial base concentration, $[B^+H]$ is the concentration of the protonated base, and $K_D$ is the dissociation constant of the ion pair $(A^\pm \cdots H{-}B^+)$.

The $k_{obs}$ values were calculated from the traces of absorbance (**3a**, $H_2O$, 468 nm, MeOH, 481 nm, MeCN + 5% MeOH, 487 nm, DMSO, 496 nm, and **3b**, $H_2O$, 496 nm) vs. time and are listed in Table 2.

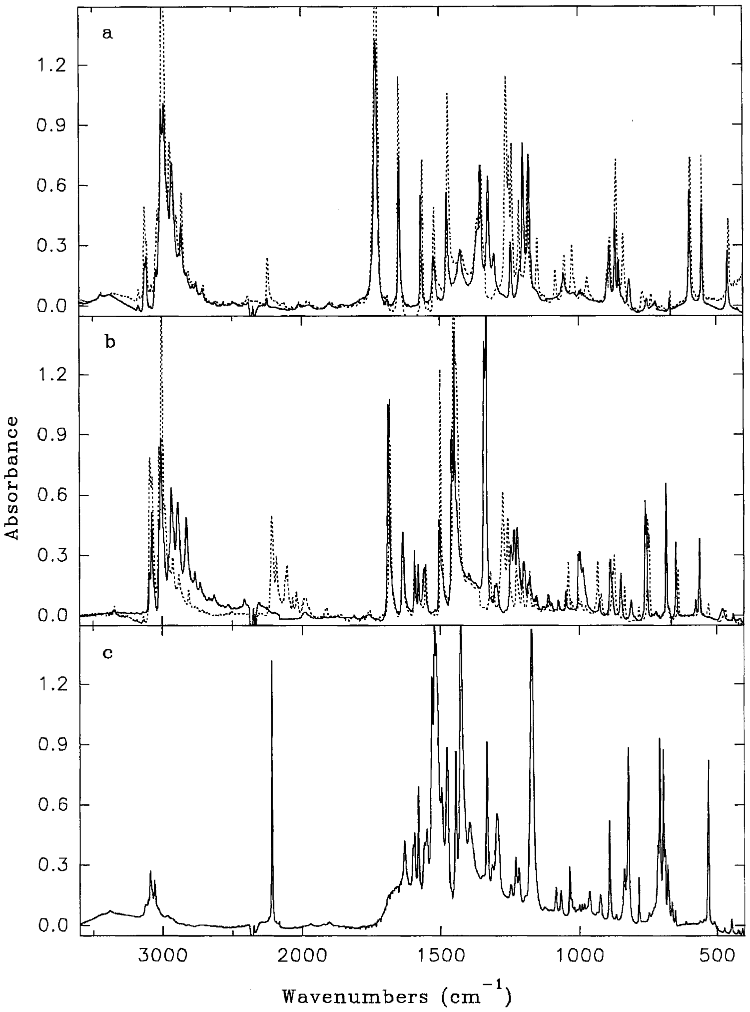

Fig. 1. FTIR spectra of *N*-acetonyl-4-cyano-pyridinium chloride, **1b·Cl**, (a), *N*-phenacyl-4-cyano-pyridinium bromide, **1a·Br** (b) and *N*-phenacyl-4-cyano-pyridinium ylide, **3a** (c) in the solid state; dotted line after deuteration).

When $k_{obs}$ was plotted vs. $[B_0]$, excellent straight lines were obtained ($r > 0.97$), where the slope gives $k$ values and the intercept, the values of $k_{-}[B^{+}H]/K_D$ (Table 2), which means that the reactions studied are correctly described by Eq. (1).

As Table 2 shows, the rate of deprotonation is solvent dependent. The fastest reaction occurs in DMSO and the slowest in methanol. The replacement of Ph group in **1a** by Me (**1b**) slows down the deprotonation ca. twice. A similar slow down process occurs in deprotonation of 4-methylpyridinium quaternary salts by a stronger base MTBD (7-methyl-1,5,7-triazabicyclo[4,4,0]dec-5-ene) in DMSO [11]. However, when CN is replaced by $N(Me)_2$ the reverse effect was found [11].

The substituent in the pyridine ring has a greater effect than that at the carbonyl group. The deprotonation of *N*-phenacyl-4-methylpyridinium bromide by a stronger base, MTBD (p$K_a$ ($CH_3CN$) = 24.17 [30], PA = 1015.5 kJ/mol [31]) is ca. 18 times slower than that of **1a** by DABCO. These data confirmed that electron-withdrawing substituents accelerate deprotonation, while electron-donating ones slow it down. A similar effect of the ring

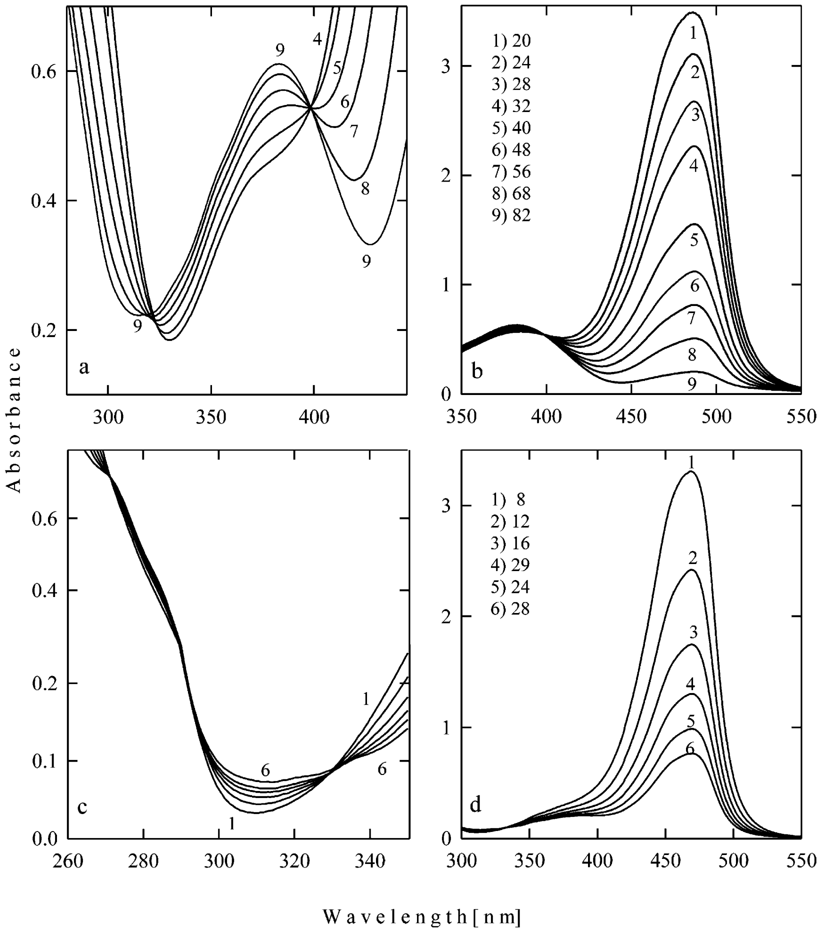

Fig. 2. Time-dependent (min) UV–Vis spectra of (a and b) **1a·Br** (1 mM) with DABCO (10 mM) in DMSO and (c and d) **1b·Cl** (1 mM) with DABCO (10 mM) in $CH_3CN$ + 5% MeOH, cell 0.5 cm.

substituents on the elimination reaction of β-proton from *N*-(2-cyanoethyl)-R-pyridinium cation in aqueous solution was observed by Bunting et al. [32].

The activation parameters (Table 3) were calculated from the Eyring equation in the form Eq. (2) [33,34]:

$$\log\frac{k}{T} = \log\frac{k_B}{h} + \frac{\Delta S^{\neq}}{2.303R} - \frac{\Delta H^{\neq}}{2.303RT}$$

$$= 10.319 + \frac{\Delta S^{\neq}}{19.148} + \frac{1000\,\Delta H^{\neq}}{19.148T} \qquad (2)$$

where $k_B = 1.380658(12) \times 10^{-23}$ J $K^{-1}$ is the Boltzmann constant, $h = 6.6260755(40) \times 10^{-34}$ J s is the Planck's constant and $R = 8.314510(70)$ J $mol^{-1}$ $K^{-1}$ is the gas constant. The $\Delta S^{\neq}$ values (Table 3) demonstrate that ylide (**3a**) in DMSO is much more solvated than in water.

### 3.3. PM3 and DFT calculations

The conformers of *N*-phenacyl-4-cyanopyridinium cation, ylide and their complexes with ammonia found by the PM3 calculations are collected in Fig. 4(a) and (b), the geometrical parameters are listed in Table 4 and the energies in Table 5. The atom numbering is given in Scheme 1. The PM3 geometries were chosen as starting structures of the DFT calculations and the obtained energies are collected in Table 6. As shown by the data of Table 5, **1a** is by 13.8 kJ/mol less stable

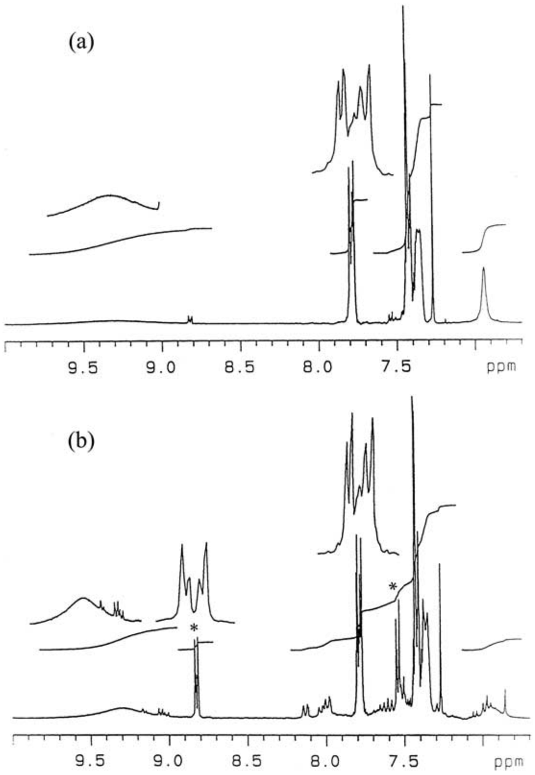

Fig. 3. The $^1H$ NMR spectra in $CDCl_3$ of **3a** (a) immediately after solution and (b) after 3.5 h; * denote chemical shifts of 4-CN-pyridine.

than **2a**(**I**) but more stable than conformer **2a**(**II**) (Fig. 4(a)). The reverse stability relation is predicted by the B3LYP computation (Table 6). An analogous reverse stability order predicted by the PM3 and B3LYP/6-31G(d,p) calculations has been reported by Zhu and Lifshitz [35] for complexation of protonated betaine with ammonia.

The PM3 calculations reproduce five complexes with ammonia (**5**–**9**) (Fig. 4(b)). Their relative energies decrease in the order **7ac** > **6ac** > **5ac** > **8ac** > **9ac** and **7bc** > **6bc** > **5bc** > **8bc** > **9bc** (Table 5). In the gas phase the molecular complexes are usually more stable than their ion pairs. Thus, the lower energies of **9ac** and **9bc** in comparison with those in **8ac** and **8bc** are surprising. Ammonia forms molecular complex in the gas phase with a much stronger acid like HCl [36]. The $O_1\cdots N_3$ distance in **9ac** is slightly shorter in comparison to that in **8ac** (Table 7) and this probably caused the lowering of the observed $E_{\mathrm{rel.}}$ in the former complex (Table 5).

The structures of **5ac** and **7ac** are the first order transition states with one imaginary frequency. Complex **6ac** has two imaginary frequencies and is a second order saddle point. For the remaining complexes (**8ac** and **9ac**) the calculated frequencies are positive. The binding energy of the $N^+H_4$/ylide (**9ac**) is 104.2 kJ/mol, which is considerably higher

Table 1
$^1H$ and $^{13}C$ NMR chemical shift (ppm) and multiplicity in DMSO-$d_6$ of **1a·Br**, **1b·Cl**, **3a** and **3b**

| | **1a·Br** | | **1b·Cl** | | **3a** | | | **3b** |
|---|---|---|---|---|---|---|---|---|
| | $^1H$ | $^{13}C$ | $^1H$ | $^{13}C$ | $^1H$ | $^1H^a$ | $^{13}C$ | $^1H$ |
| *Pyridine ring* | | | | | | | | |
| α | 9.35, d | 147.65 | 9.39, d | 147.05 | 9.58, b | 9.32, b | 140.89 | 9.27, b |
| β | 8.84, d | 130.74 | 8.80, d | 130.35 | 7.83, m | 7.37, d | 126.25 | 7.72, d |
| γ | | 127.85 | | 127.34 | | | 105.64 | |
| *Phenyl ring* | | | | | | | | |
| Ipso | | 133.35 | | | | | 128.94 | |
| *o* | 8.08, d | 128.38 | | | 7.83, m | 7.80, d | 128.75 | |
| *m* | 7.67, t | 129.23 | | | 7.45, m | 7.40, m | 128.19 | |
| *p* | 7.81, t | 134.91 | | | 7.45, m | 7.40, m | 129.93 | |
| $CH_2$/CH | 6.67, s | 67.13 | 6.13, s | 68.82 | 7.45, m | 6.85, b | 102.78 | 6.67, s |
| CO | | 189.59 | | 198.37 | | | 173.45 | |
| CN | | 114.89 | | 114.67 | | | 117.31 | |
| $CH_3$ | | | 2.35, s | 27.22 | | | | 1.91, s |

s = singlet, d = doublet, t = triplet, m = multiplet, b = broad.

[a] In $CDCl_3$.

Table 2
Kinetic data and activation parameters for the deprotonation of 4-CN–$C_5H_4N^+$–$CH_2$–COPh·$Br^-$ (**1a·Br**) and 4-CN–$C_5H_4N^+$–$CH_2$–COMe·$Cl^-$ (**1b·Cl**)

| Solvent | $T$ (°C) | $k_{obs}$ ($s^{-1}$) | | | | | $k$ ($M^{-1}$ $s^{-1}$)$10^{-4}$ | $k_-$ [$B^+H$]/$K_D$ ($s^{-1}$) |
|---|---|---|---|---|---|---|---|---|
| *4-CN–$C_5H_4N^+$–$CH_2$–COPh·$Br^-$* | | | | | | | | |
| $B_0$ (M) × $10^{-4}$ | | 1 | 2 | 3 | 4 | 5 | | |
| MeOH | 25 | 7.2(1) | 12.5(1) | 18.0(2) | 22.5(2) | 25.1(3) | 4.5(3) | 3.4(1.0) |
| | 30 | 13.4(1) | 18.1(1) | 24.0(2) | 32.0(2) | 37.3(9) | 6.1(2) | 6.5(8) |
| | 35 | 19.6(8) | 29.4(5) | 35.4(7) | 45.4(9) | 52.5(9) | 8.1(3) | 12.0(9) |
| | 40 | 27.6(2) | 38.8(1) | 52.0(3) | 61.8(4) | 72.4(5) | 11.1(4) | 16.9(1.2) |
| MeCN + 5%MeOH | 25 | 13.0(1) | 19.9(1) | 23.8(1) | 30.2(1) | 36.6(1) | 5.7(3) | 7.4(9) |
| | 30 | 21.4(1) | 30.4(1) | 37.6(1) | 45.4(1) | 54.0(2) | 8.0(2) | 13.7(6) |
| | 35 | 32.2(1) | 40.2(1) | 50.4(2) | 61.4(2) | 73.3(2) | 10.3(4) | 20.5(1.4) |
| | 40 | 47.2(2) | 55.1(2) | 66.6(2) | 83.4(3) | 98.3(4) | 13.0(10) | 30.9(3.3) |
| DMSO | 25 | | 207.4(3) | 300.6(1.1) | 381.7(2.1) | 428.7(2.2) | 74.4(73) | 68.7(27.0) |
| | 30 | | 273.2(3) | 375.4(1.4) | 469.5(2.3) | 525.6(3.3) | 84.8(77) | 113.7(28.4) |
| | 35 | | 323.4(4) | 454.8(1.3) | 566.2(3.1) | 622.5(2.5) | 100.8(120) | 138.4(44.2) |
| | 40 | | 407.3(3) | 533.6(2.4) | 652.4(2.5) | 745.7(4.5) | 113.3(54) | 187.6(19.9) |
| $H_2O$ | 25 | 24.4(1) | 34.5(1) | 42.3(1) | 53.4(1) | 58.0(2) | 8.6(5) | 16.7(1.8) |
| | 30 | 32.8(1) | 43.3(1) | 57.0(2) | 69.0(2) | 80.7(3) | 12.1(2) | 20.1(8) |
| | 35 | 42.0(3) | 58.7(3) | 76.2(4) | 94.0(5) | 111.0(6) | 17.3(1) | 24.3(4) |
| | 40 | 56.8(3) | 84.5(4) | 107.8(6) | 127.0(7) | 156.0(8) | 24.1(9) | 34.1(2.9) |
| *4-CN–$C_5H_4N^+$–$CH_2$–COMe·$Cl^-$* | | | | | | | | |
| $B_0$ (M) × $10^{-4}$ | | 2 | 3 | 4 | 5 | 6 | | |
| $H_2O$ | 25 | 21.0(1) | 25.3(1) | 30.6(1) | 33.5(2) | 38.5(2) | 4.3(1) | 12.1(0.4) |
| | 30 | 30.0(3) | 34.1(2) | 39.1(2) | 44.1(2) | 50.3(3) | 5.3(2) | 18.3(1.0) |
| | 35 | 44.0(3) | 50.8(3) | 56.2(3) | 62.3(4) | 69.7(4) | 6.6(2) | 29.2(0.8) |
| | 40 | 56.5(6) | 64.2(4) | 71.3(5) | 80.6(7) | 89.2(6) | 8.4(2) | 38.3(0.7) |

than the binding energy of 49.4 kJ/mol for $NH_3$/enol (**8ac**). The difference in the binding energies between **5ac** and **6ac** is 5.9 kJ/mol, while between **7ac** and **5ac** is 9.2 kJ/mol (Table 5).

When DABCO is used for deprotonation, the PM3 method reproduces only three complexes with a reasonably increasing relative energy, **8ad** < **5 ad** < **9ad** and **8bd** < **9bd** ≈ **5bd** (Table 5). The decrease of the number of complexes may be explained by a larger volume of the DABCO molecule.

Although DABCO is a weaker base in water and slightly stronger in the gas phase, than ammonia (p$K_a$ = 9.36 (20°), PA = 853.5 kJ/mol [21]), the calculated complexation energies ($E_{COMPL}$) do not reflect this difference (Table 5). A replacement of Ph group by Me has little effect on the complexation energy. This suggests that the coupling between the phenyl ring and the oxygen atom in *N*-phenacyl-4-cyanopyridinium cation and ylide is negligible.

According to the B3LYP/6-31G(d,p) calculations only two complexes, **5ac** and **8ac** are formed, whose

Table 3
Activation parameters for the deprotonations of 4-CN–$C_5H_4N^+$–$CH_2$–COPh·$Br^-$ (**1a·Br**) and 4-CN–$C_5H_4N^+$–$CH_2$–COMe·$Cl^-$ (**1b·Cl**) with 1,4-diazabicyclo[2,2,2]octane (DABCO)

| Solvent | $\Delta H^{\neq}$ (kJ/mol) | $\Delta S^{\neq}$ (J $mol^{-1}$ $deg^{-1}$) | $\Delta G^{\neq}$ (kJ $mol^{-1}$) |
|---|---|---|---|
| *4-CN–$C_5H_4N^+$–$CH_2$–COPh·$Br^-$* | | | |
| MeOH | 43.7(1.0) | −9(3) | 46.5(1.0) |
| MeCN + 5%MeOH | 39.6(2.1) | −21(7) | 45.8(2.1) |
| DMSO | 19.8(1.1) | −66(4) | 39.5(1.1) |
| $H_2O$ | 50.9(0.4) | 20(2) | 44.9(0.4) |
| *4-CN–$C_5H_4N^+$–$CH_2$–COMe·$Cl^-$* | | | |
| $H_2O$ | 32.5(1.0) | −47(3) | 46.6(1.0) |

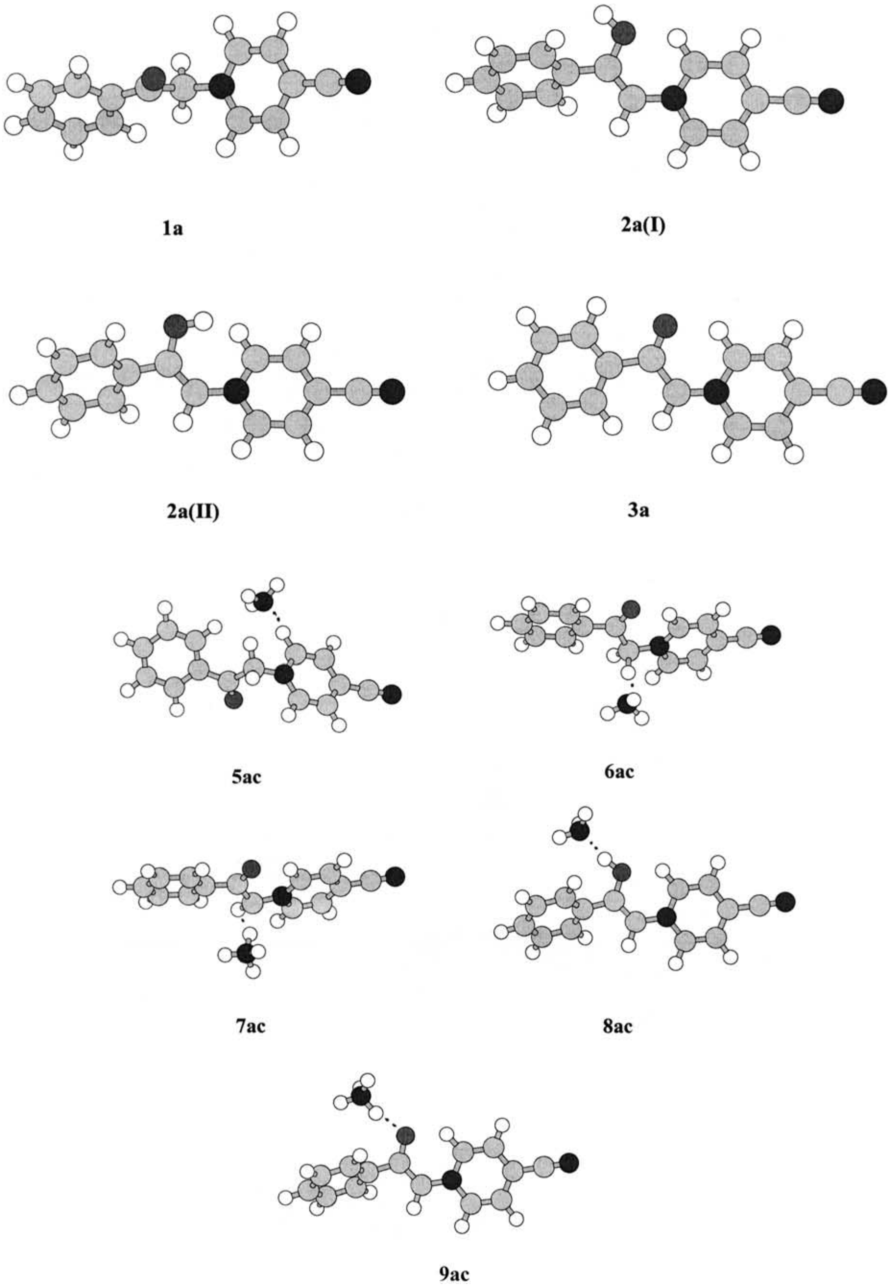

**1a** **2a(I)**

**2a(II)** **3a**

**5ac** **6ac**

**7ac** **8ac**

**9ac**

Fig. 4. The optimized PM3 structures of (a) **1a**–**3a** and (b) **5ac**–**9ac**.

energies are at the minima on the potential energy surface, as all their frequencies are positive. The BLYP calculations reproduce also complex **6ac** (Tables 4 and 6, Fig. 4(b)).

As shown by the data in Table 4, the majority of bond lengths calculated by the PM3 method for **1a**, **2a** and **3a** are slightly longer in comparison to the corresponding bonds reproduced by the B3LYP

Table 4
Bond lengths (Å), bond and torsion angles (°) of 1-phenacyl-4-cyanopyridinium cations (**1a**, **2a**(**I**)) and 1-phenacyl-4-cyanopyridinium ylide (**3a**) calculated by B3LYP and PM3 level of theory

| Parameter<br>Bond | **1a**<br>B3LYP | **1a**<br>PM3 | **2a**(**I**)<br>B3LYP | **2a**(**I**)<br>PM3 | **3a**<br>B3LYP | **3a**<br>BLYP | **3a**<br>PM3 | Parameter<br>Angle | **1a**<br>B3LYP | **1a**<br>PM3 | **2a**(**I**)<br>B3LYP | **2a**(**I**)<br>PM3 | **3a**<br>B3LYP | **3a**<br>BLYP | **3a**<br>PM3 |
|---|---|---|---|---|---|---|---|---|---|---|---|---|---|---|---|
| $N_1$···$O_1$ | 2.666 | 2.762 | 2.936 | 2.872 | 2.925 | 2.952 | 2.881 | | | | | | | | |
| $N_1$–$C_2$ | 1.356 | 1.376 | 1.369 | 1.376 | 1.388 | 1.404 | 1.392 | $N_1$–$C_2$–$C_3$ | 120.8 | 120.5 | 121.2 | 121.1 | 121.2 | 121.2 | 121.7 |
| $N_1$–$C_6$ | 1.357 | 1.377 | 1.372 | 1.381 | 1.387 | 1.402 | 1.395 | $N_1$–$C_6$–$C_5$ | 121.0 | 120.5 | 121.9 | 120.9 | 122.4 | 122.3 | 121.4 |
| $N_1$–$C_8$ | 1.473 | 1.487 | 1.417 | 1.426 | 1.372 | 1.383 | 1.357 | $N_1$–$C_8$–$C_9$ | 109.9 | 113.4 | 128.4 | 126.6 | 125.1 | 125.3 | 124.5 |
| $C_2$–$C_3$ | 1.383 | 1.391 | 1.381 | 1.392 | 1.376 | 1.383 | 1.381 | $C_2$–$N_1$–$C_6$ | 120.7 | 120.4 | 118.8 | 119.5 | 117.5 | 117.4 | 118.0 |
| $C_3$–$C_4$ | 1.402 | 1.401 | 1.402 | 1.399 | 1.406 | 1.420 | 1.402 | $N_2$–$C_7$–$C_4$ | 179.9 | 180.0 | 180.0 | 180.0 | 179.8 | 179.9 | 179.9 |
| $C_4$–$C_5$ | 1.407 | 1.402 | 1.406 | 1.402 | 1.409 | 1.422 | 1.398 | $C_2$–$C_3$–$C_4$ | 119.3 | 119.4 | 120.4 | 119.4 | 121.6 | 121.8 | 119.7 |
| $C_5$–$C_6$ | 1.379 | 1.390 | 1.375 | 1.389 | 1.370 | 1.378 | 1.385 | $C_3$–$C_4$–$C_5$ | 119.0 | 119.7 | 118.0 | 119.5 | 116.8 | 116.6 | 119.3 |
| $C_8$–$C_9$ | 1.564 | 1.541 | 1.362 | 1.369 | 1.429 | 1.439 | 1.455 | $C_4$–$C_5$–$C_6$ | 119.1 | 119.5 | 119.7 | 119.5 | 120.6 | 116.6 | 119.8 |
| $C_9$–$O_1$ | 1.220 | 1.214 | 1.450 | 1.352 | 1.249 | 1.264 | 1.233 | $C_8$–$C_9$–$O_1$ | 117.7 | 119.5 | 120.8 | 118.8 | 124.4 | 124.2 | 122.1 |
| $C_4$–$C_7$ | 1.431 | 1.420 | 1.429 | 1.421 | 1.424 | 1.427 | 1.419 | $C_7$–$C_4$–$C_3$ | 120.6 | 120.2 | 121.1 | 120.3 | 121.8 | 121.9 | 120.4 |
| $C_7$–$N_2$ | 1.162 | 1.159 | 1.163 | 1.159 | 1.165 | 1.179 | 1.160 | $C_8$–$C_9$–$C_{10}$ | 117.8 | 115.3 | 121.5 | 118.8 | 116.7 | 116.8 | 116.8 |
| $C_9$–$C_{10}$ | 1.471 | 1.475 | 1.472 | 1.468 | 1.506 | 1.516 | 1.493 | $O_1$–$C_8$–$C_{1'}$ | 124.5 | 125.2 | 120.8 | 119.6 | 118.9 | 119.0 | 121.0 |
| $C_{10}$–$C_{11}$ | 1.409 | 1.398 | 1.408 | 1.401 | 1.403 | 1.414 | 1.398 | $C_9$–$C_{10}$–$C_{11}$ | 117.5 | 119.5 | 119.2 | 120.0 | 117.2 | 117.2 | 119.6 |
| $C_{11}$–$C_{12}$ | 1.389 | 1.392 | 1.392 | 1.389 | 1.392 | 1.402 | 1.389 | $C_8$–$C_{10}$–$C_{15}$ | 122.9 | 120.9 | 121.3 | 120.0 | 123.9 | 117.2 | 121.3 |
| $C_{12}$–$C_{13}$ | 1.399 | 1.390 | 1.397 | 1.393 | 1.397 | 1.407 | 1.391 | $C_{10}$–$C_{11}$–$C_{12}$ | 120.1 | 119.9 | 120.1 | 119.8 | 120.7 | 120.7 | 120.3 |
| $C_{13}$–$C_{14}$ | 1.398 | 1.395 | 1.397 | 1.392 | 1.396 | 1.406 | 1.390 | $C_{10}$–$C_{15}$–$C_{14}$ | 120.0 | 120.2 | 120.0 | 119.8 | 120.5 | 120.6 | 120.4 |
| $C_{14}$–$C_{15}$ | 1.391 | 1.386 | 1.392 | 1.390 | 1.394 | 1.404 | 1.391 | $C_{11}$–$C_{12}$–$C_{13}$ | 120.0 | 120.3 | 120.1 | 120.2 | 120.1 | 120.1 | 120.2 |
| $C_{15}$–$C_{10}$ | 1.408 | 1.401 | 1.406 | 1.399 | 1.403 | 1.415 | 1.398 | $C_{12}$–$C_{13}$–$C_{14}$ | 120.4 | 120.0 | 120.1 | 120.0 | 119.7 | 119.7 | 119.8 |
| r.m.s | | 0.011 | | 0.024 | | 0.08 | 0.014 | $C_{13}$–$C_{14}$–$C_{15}$ | 119.9 | 120.0 | 120.2 | 120.2 | 120.1 | 120.2 | 120.2 |
| Torsion | | | | | | | | $C_{11}$–$C_{10}$–$C_{15}$ | 119.6 | 119.6 | 119.5 | 119.9 | 118.8 | 118.7 | 119.1 |
| $N_1$–$C_8$–$C_9$–$O_1$ | −14.2 | 14.2 | −5.1 | −0.5 | −2.4 | −2.3 | 1.2 | H–$C_8$–$N_1$ | 108.3 | 110.0 | 113.3 | 115.8 | 113.9 | 113.6 | 118.4 |
| $C_2$–$N_1$–$C_8$–$C_9$ | 63.9 | −89.4 | 3.8 | −0.5 | −1.4 | −1.5 | −0.3 | | 108.8 | 110.6 | | | | | |
| $C_6$–$N_1$–$C_8$–$C_9$ | −110.4 | 89.0 | −177.2 | 179.8 | 178.6 | 178.5 | 179.7 | H–$C_8$–$C_9$ | 111.9 | 108.3 | 118.3 | 117.8 | 121.0 | 121.3 | 117.0 |
| $C_{10}$–$C_9$–$C_8$–$N_1$ | 167.3 | −166.5 | 176.9 | 179.7 | 179.2 | 179.3 | −178.5 | | 109.6 | 108.7 | | | | | |
| $C_2$–$N_1$–$C_8$–$O_1$ | 40.3 | −59.5 | −1.8 | −0.9 | −3.2 | −3.1 | 0.8 | r.m.s | | 1.5 | | 1.2 | | 0.9 | 1.9 |
| $C_{15}$–$C_{10}$–$C_9$–$O_1$ | −177.2 | 83.9 | 143.4 | 178.8 | 175.8 | 179.7 | −179.5 | | | | | | | | |
| $C_8$–$C_9$–$O_1$H | | | 169.7 | 179.6 | | | | | | | | | | | |
| $C_{10}$–$C_9$–$O_1$H | | | −12.2 | −0.7 | | | | | | | | | | | |

Table 5
Total energies (kJ/mol), enthalpies of formation (kJ/mol), relative energies (kJ/mol) and dipole moments (Debye) calculated by the PM3 method of investigated compounds

| Compound | $\Delta H_f$ | $E_{rel.}$ | $E_{COMPL}$ | $\mu$ | Compound | $\Delta H_f$ | $E_{rel}$ | $E_{COMPL}$ | $\mu$ |
|---|---|---|---|---|---|---|---|---|---|
| *N-phenacyl* | | | | | *N-acetonyl* | | | | |
| **1a** | 925.5 | 13.8 | | 4.94 | **1b** | 788.7 | 11.3 | | 5.89 |
| **2a(I)** | 911.7 | 0 | | 1.20 | **2b(I)** | 777.4 | 0 | | 6.79 |
| **2a(II)** | 943.9 | 32.2 | | 1.66 | **2b(II)** | 805.0 | 27.6 | | 3.74 |
| **3a** | 297.9 | | | 4.12 | **3b** | 152.3 | 0 | | 3.94 |
| **5ac** | 864.3 | 28.9 | −48.1 | 4.87 | **5bc** | 727.2 | 30.5 | −48.5 | 6.68 |
| **6ac** | 870.3 | 34.7 | −42.3 | 5.95 | **6bc** | 731.8 | 35.1 | −43.9 | 6.76 |
| **7ac** | 882.4 | 46.9 | −57.3 | 10.55 | **7bc** | 745.2 | 48.5 | −48.9 | 12.4 |
| **8ac** | 849.3 | 13.8 | −49.4 | 2.82 | **8bc** | 711.7 | 15.1 | −77.4 | 7.62 |
| **9ac** | 835.5 | 0 | −104.2 | 13.30 | **9bc** | 696.6 | 0 | −97.5 | 17.4 |
| **5ad** | 885.7 | 11.7 | −51.5 | 5.45 | **5bd** | 760.2 | 23.0 | −40.2 | 8.59 |
| **8ad** | 877.8 | 0 | −45.6 | 6.06 | **8bd** | 737.2 | 0 | −51.9 | 6.56 |
| **9ad** | 898.7 | 18.0 | −88.3 | 6.52 | **9bd** | 759.4 | 22.2 | −82.0 | 8.35 |
| $NH_3$ | −13.0 | | | 1.55 | DABCO | 11.7 | | | 0.00 |
| $NH_4$ | 641.8 | | | 0.00 | DABCOH | 689.1 | | | 5.36 |

calculations. For **3a** the bond lengths calculated by BLYP are slightly longer in comparison to the values obtained by B3LYP and PM3 methods. No systematic differences have been observed for the bond angles. The formation of ylide **3a** from cation **1a** causes the following geometrical changes: (i) the $N_1–C_8$ and $C_8–C_9$ bonds become shorter ca. 0.1 Å; (ii) the $C_9–O_1$ bond becomes up to 0.03 Å longer; (iii) the intramolecular $N_1\cdots O_1$ distance elongates ca. 0.1 Å (B3LYP) and 0.12 Å (PM3). The $N_1–C_8–C_9–O_1$ moiety in **1a** is perpendicular, while in **2a** and **3a** it is coplanar with the pyridine ring plane. The $C_8–C_9$ in **1a** is a typical single bond, in **2a** it is a typical double bond, while in **3a** it is between a single and a double bond. All the above data indicate that in **3a** there is a strong electron coupling between the pyridine ring and the oxygen atom through bonds, while in **1a** there is an electrostatic interaction between the oppositely charged nitrogen and oxygen atoms via space. Interesting differences between the B3LYP and PM3 data are observed for the torsion angles (Table 4), which indicate dissimilarity of their conformations.

The geometrical parameters for **1b**, **2b** and **3b** listed in Table 8 are very similar to these for **1a**, **2a** and **3a** collected in Table 4. Thus *N*-phenacyl- and *N*-acetonyl-4-cyano-pyridinium cations and ylides have similar conformation, respectively.

The DABCO complexes **8ad** and **8bd** have the lowest energies (Table 5). This suggests that ylides are formed by abstraction of hydrogen atom from the enolic form (**2a**, **2b**) via complex **8** (Scheme 3).

Table 6
Total energies (in hartrees), relative energies (kJ/mol) and dipole moments (Debye) of investigated compounds calculated by DFT methods

| Compound | Method | Energy (a.u.) | $E_{rel.}$ | $E_{HB}$ | $\mu$ |
|---|---|---|---|---|---|
| **1a** | B3LYP | −724.599633 | 0 | | 4.38 |
| | BLYP | −724.339333 | | | 4.23 |
| **2a(I)** | B3LYP | −724.590666 | 23.4 | | 2.62 |
| **3a** | B3LYP | −724.203651 | | | 4.48 |
| | BLYP | −723.947487 | | | 4.55 |
| **5ac** | B3LYP | −781.179102 | 15.1 | −57.0 | 5.48 |
| **6ac** | BLYP | −780.886634 | | | 5.53 |
| **8ac** | B3LYP | −781.184868 | 0 | −95.6 | 5.26 |
| | BLYP | −780.896082 | | | 6.06 |
| **1b** | B3LYP | −532.850504 | 0 | | 6.03 |
| **2b(I)** | B3LYP | −532.844801 | 15.1 | | 7.40 |
| **3b** | B3LYP | −532.461362 | | | 4.39 |
| | BLYP | −532.281287 | | | 4.53 |
| $NH_3$ | B3LYP | −56.557768 | | | 1.85 |
| $NH_4$ | B3LYP | −56.905864 | | | 0.00 |

Table 7
Selected distances (Å), angles and torsion angles (deg) derived by the PM3, B3LYP and BLYP calculations for 1-phenacyl-4-cyanopyridine derivatives from Scheme 2

| Parameter | **5ac**<br>B3LYP | **5ac**<br>PM3 | **6ac**<br>BLYP | **6ac**<br>PM3 | **7ac**<br>PM3 | **8ac**<br>B3LYP | **8ac**<br>PM3 | **9ac**<br>PM3 | **5ad**<br>PM3 | **8ad**<br>PM3 | **9ad**<br>PM3 |
|---|---|---|---|---|---|---|---|---|---|---|---|
| $C_9$–$O_1$ | 1.130 | 1.213 | 1.235 | 1.216 | 1.229 | 1.335 | 1.334 | 1.265 | 1.213 | 1.333 | 1.261 |
| $N_1\cdots O_1$ | 2.673 | 2.781 | 2.711 | 2.763 | 2.874 | 2.963 | 2.874 | 2.906 | 2.778 | 2.865 | 2.904 |
| $N_1$–$C_8$ | 1.474 | 1.487 | 1.479 | 1.479 | 1.420 | 1.415 | 1.420 | 1.389 | 1.487 | 1.421 | 1.386 |
| $C_8$–$C_9$ | 1.558 | 1.537 | 1.575 | 1.529 | 1.479 | 1.388 | 1.375 | 1.410 | 1.537 | 1.377 | 1.414 |
| $C_9$–$C_{10}$ | 1.475 | 1.478 | 1.480 | 1.479 | 1.487 | 1.490 | 1.473 | 1.490 | 1.478 | 1.473 | 1.491 |
| $C_8\cdots N_3$ | | | 3.224 | 2.912 | 2.725 | | | | | | |
| $(C_8)H\cdots N_3$ | | | 2.111 | 1.742 | 1.650 | | | | | | |
| $C_8H\cdots N_3$ | | | 172.9 | 177.1 | 172.9 | | | | | | |
| $C_6\cdots N_3$ | 3.244 | 2.892 | | | | | | | 2.903 | | |
| $(C_6)H\cdots N_3$ | 2.158 | 1.728 | | | | | | | 1.740 | | |
| $C_6 \cdot H\cdots N_3$ | 171.3 | 177.9 | | | | | | | 177.9 | | |
| $O_1\cdots N_3$ | | | 2.711 | | | 2.963 | 2.696 | 2.682 | | 2.699 | 2.750 |
| $O_1\cdots HN_3/O_1H\cdots N_3$ | | | | | | 1.537 | 1.722 | 1.708 | | 1.740 | 1.713 |
| $O_1H \cdot N_3$ | | | | | | 172.1 | 167.4 | 155.7 | | 162.7 | 172.7 |
| $C_8$–$C_9$–$O_1$ | 118.3 | 120.3 | 118.1 | 119.9 | 121.5 | 121.8 | 119.6 | 123.9 | 120.4 | 119.0 | 123.9 |
| $C_{10}$–$C_8$–$O_1$ | 124.0 | 124.8 | 123.7 | 124.3 | 121.7 | 119.5 | 120.2 | 119.0 | 124.8 | 121.3 | 119.4 |
| $N_1$–$C_8$–$C_9$–$O_1$ | 11.7 | 13.4 | −21.7 | −17.8 | −24.3 | −4.3 | −0.3 | 1.0 | −10.0 | −1.5 | 1.5 |
| $C_2$–$N_1$–$C_8$–$C_9$ | −63.7 | −82.8 | 64.2 | 80.7 | 22.2 | 2.7 | −0.8 | −0.4 | 76.0 | 3.4 | 0.9 |
| $C_6$–$N_1$–$C_7$–$C_8$ | 111.6 | 96.7 | −109.9 | −98.3 | −160.6 | −177.7 | 179.1 | 179.6 | −103.3 | −175.7 | −179.1 |
| $C_{10}$–$C_9$–$C_8$–$N_1$ | −169.3 | −167.4 | 160.8 | 163.2 | 159.3 | 178.6 | −179.8 | −179.0 | 170.9 | 178.5 | −178.6 |
| $C_2$–$N_1\cdots C_9$–$O_1$ | −42.2 | −55.7 | 34.4 | 50.8 | | −1.5 | −0.9 | | 53.5 | 1.6 | 2.0 |
| $C_{15}$–$C_{10}$–$C_9$–$O_1$ | 176.5 | −148.7 | −179.6 | 153.3 | 158.6 | 140.2 | 128.5 | 122.2 | 147.9 | 132.0 | 114.2 |
| $C_8$–$C_9$–$O_1$–H | | | | | | 161.6 | 176.6 | | | 177.5 | |
| $C_{10}$ $C_9$–$O_1$–H | | | | | | −40.6 | −3.9 | | | −2.5 | |
| $C_{11}$–$C_{10}$–$C_9$–$O_1$ | −2.8 | 30.2 | 2.8 | −25.1 | −18.9 | −40.6 | −52.3 | −58.6 | −31.1 | −48.3 | −66.5 |

Table 8
Selected distances (Å), angles and torsion angles (deg) calculated by the PM3 method of 1-acetonyl-4-cyanopyridine derivatives from Scheme 2

| Parameters | **1b** | **2b(I)** | **3b** | **5bc** | **6bc** | **7bc** | **8bc** | **9bc** | **5bd** | **8bd** | **9bd** |
|---|---|---|---|---|---|---|---|---|---|---|---|
| $C_9-O_1$ | 1.211 | 1.351 | 1.231 | 1.211 | 1.213 | 1.226 | 1.333 | 1.264 | 1.211 | 1.335 | 1.260 |
| $N_1\cdots O_1$ | 2.765 | 2.874 | 2.874 | 2.779 | 2.770 | 2.886 | 2.871 | 2.903 | 2.775 | 2.864 | 2.899 |
| $C_8-N_1$ | 1.489 | 1.429 | 1.357 | 1.489 | 1.480 | 1.422 | 1.422 | 1.387 | 1.488 | 1.423 | 1.385 |
| $C_8-C_9$ | 1.539 | 1.366 | 1.455 | 1.536 | 1.527 | 1.478 | 1.374 | 1.412 | 1.536 | 1.373 | 1.416 |
| $C_9-C_{10}$ | 1.496 | 1.489 | 1.503 | 1.497 | 1.497 | 1.502 | 1.491 | 1.502 | 1.497 | 1.491 | 1.503 |
| $C_8\cdots N_3$ | | | | | 2.909 | 2.726 | | | | | |
| $(C_8)H\cdots N_3/C_8\cdots HN_3^+$ | | | | | 1.741 | 1.648 | | | | | |
| $C_8 \cdot H \cdot N_3$ | | | | | 174.5 | 174.1 | | | | | |
| $C_6\cdots N_3$ | | | | 2.889 | | | | | 2.859 | | |
| $(C_6)H\cdots N_3$ | | | | 1.725 | | | | | 1.748 | | |
| $C_6 \cdot H \cdot N_3$ | | | | 174.9 | | | | | 157.2 | | |
| O–H | | 0.953 | | | | | 0.989 | | | 0.988 | |
| $O_1\cdots N_3$ | | | | 4.658 | | | 2.698 | 2.658 | 4.953 | 2.719 | 2.745 |
| $O_1\cdots HN_3/O_1H\cdots N_3$ | | | | | | | 1.722 | 1.712 | | 1.734 | 1.712 |
| $O_1HN_3$ | | | | | | | 168.4 | 150.6 | | 174.7 | 171.0 |
| $C_8-C_9-O_1$ | 120.4 | 118.9 | 123.1 | 120.8 | 120.9 | 122.1 | 119.3 | 123.3 | 120.8 | 119.2 | 123.3 |
| $C_{10}-C_9-O_1$ | 125.4 | 120.1 | 121.9 | 125.0 | 124.7 | 122.3 | 121.1 | 120.3 | 125.0 | 120.5 | 120.6 |
| $N_1-C_7-C_8-O_1$ | 2.3 | −0.0 | −0.0 | −3.8 | 8.6 | 28.0 | −0.1 | −0.1 | 0.6 | −0.3 | 0.6 |
| $C_2-N_1-C_8-C_9$ | −90.3 | −0.4 | −0.2 | −84.3 | 101.8 | −24.0 | 0.3 | 0.1 | −85.7 | 6.0 | 2.5 |
| $C_6-N_1-C_8-C_9$ | 88.6 | −179.8 | −180.0 | 95.3 | −77.6 | 158.7 | −179.7 | −179.8 | 93.4 | −174.2 | −177.3 |
| $C_{10}-C_9-C_8-N_1$ | −177.6 | 180.0 | 180.0 | 176.3 | −171.8 | −154.2 | 179.8 | 179.9 | 179.3 | 179.1 | −179.6 |
| $C_2-N_1\cdots C_9-O_1$ | −70.7 | −0.4 | −0.2 | −71.7 | 88.6 | 3.2 | −0.2 | 0.0 | −68.7 | 4.9 | 2.7 |
| $C_8-C_9-O_1-H$ | | −179.9 | | | | | 179.6 | | | 177.6 | |
| $C_{10}-C_9-O_1-H$ | | 0.1 | | | | | −0.3 | | | −1.8 | |

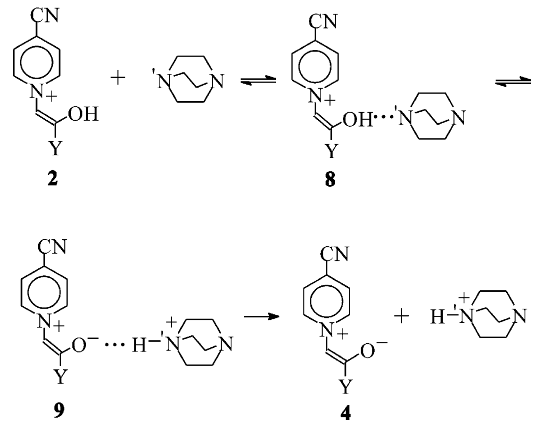

Scheme 3.

## 4. Summary

The deprotonation of **1a** and **1b** with DABCO in protic and aprotic solvents has been investigated by kinetic, UV, $^1H$ and $^{13}C$ NMR spectroscopy, PM3 and B3LYP/6-31G(d,p) calculations. The $k_{obs}$ data fit well Eq. (1). The UV–Vis spectra of **1a** and **1b** show solvent dependent isosbestic points, which suggests that the decomposition reactions of ylides are very probably uniform. Two mechanisms for ylide decomposition reaction are proposed.

The easy replacement of $N^+CH_2$ hydrogens in **1a·Br** and **1b·Cl** by deuterium in $D_2O$ or $CH_3OD$ solutions and the calculation results show that the cations investigated are in a tautomeric equilibrium with enols (**1a** → **2a** and **1b** → **2b**). The number of complexes depends on the applied method of calculations and the base used. The ordering of the complexes according to their stability predicted by the methods PM3 and B3LYP is reverse. The PM3 calculations predict five complexes with ammonia and three with DABCO. The B3LYP calculations reproduce only two complexes with ammonia, while the BLYP three.

The complexation energy ($E_{COMPL}$) estimated from the PM3 calculations decreases in the order: **9ac** $\gg$ **7ac** > **8ac** > **5ac** > **6ac** and **9bc** > **8bc** > **7 bc** > **5bc** > **6bc**. In the complexes with DABCO the binding energy is slightly lower in comparison to these in complexes with ammonia and decreases in the order **9ad** > **5ad** > **8ad** and **9bd** > **8bd** > **5bd**. The replacement of Ph group by Me one was found to cause an insignificant effect. This suggests that electron coupling occurred mainly between the pyridine ring and the oxygen.

Ylides are formed by abstraction of the hydroxyl proton from enolic form (**2a**,**2b**) via complex **8**.

## Acknowledgments

We acknowledge the Poznań Supercomputing and Network Centre for access to their computers.

## References

[1] W.G. Phillips, K.W. Ratts, J. Org. Chem. 35 (1970) 3144.
[2] A.R.E. Carey, R.A. More O'Ferrall, B.A. Murray, J. Chem. Soc. Perkin Trans. 2 (1993) 2297.
[3] E.P. Serjant, B. Dempsey, Ionisation Constants of Organic Acids in Aqueous Solutions, IUPAC Chemical data, Series No. 23, Pergamon Press, Oxford, 1979.
[4] G. Gilli, V. Bertolasi, V. Ferretti, P. Gilli, Acta Crystallogr. B49 (1993) 584.
[5] C. Reichardt, Solvent Effects in Organic Chemistry, Verlag, Weinheim, 1979, p. 61.
[6] M.T. Rogers, J.L. Burdett, Can. J. Chem. 43 (1965) 1516.
[7] W.P. Litvinov, Zh. Org. Khim. 29 (1993) 2070.
[8] W.P. Litvinov, Zh. Org. Khim. 30 (1994) 1572.
[9] W.P. Litvinov, Zh. Org. Khim. 31 (1995) 1441.
[10] W.P. Litvinov, A.M. Shestopalov, Zh. Org. Khim. 33 (1997) 975.
[11] Z. Dega-Szafran, G. Schroeder, M. Szafran, A. Szwajca, B. Łęska, M. Lewandowska, J. Mol. Struct. 555 (2000) 31.
[12] J.J.P. Stewart, J. Comput. Chem. 10 (1989) 209.
[13] AMPAC 6.0, Semichem, Shawnee, KS 66216, 1998.
[14] M.J. Fritsch, G.W. Trucks, H.B. Schlegel, G.E. Scuseria, M.A. Robb, J.R. Cheeseman, V.G. Zakrzewski, A.J. Jr. Montgomery, R.E. Stratmann, J.C. Burant, S. Dapprich, J.M. Millam, A.D. Daniels, K.N. Kudin, M.C. Strain, O. Farkas, J. Tomasi, V. Barone, M. Cossi, R. Cammi, B. Mennucci, C. Pomelli, C. Adamo, S. Clifford, J. Ochterski, G.A. Petersson, P.Y. Ayala, Q. Cui, K. Morokuma, D.K. Malick, A.D. Rabuck, K. Raghavachari, J.B. Foresman, J. Cioslowski, J.V. Ortiz, B.B. Stefanov, G. Liu, A. Liashenko, P. Piskorz, I. Komaromi, R. Gomperts, R.L. Martin, D.J. Fox, T. Keith, M.A. Al-Laham, C.Y. Peng, A. Nanayakkara, C. Gonzalez, M. Challacombe, P.M.W. Gill, B. Johnson, W. Chen, M.W. Wong, J.L. Andres, C. Gonzalez, M. Head-Gordon, E.S. Replogle, J.A. Pople, GAUSSIAN 98, Revision A.6, Gaussian, Pittsburg, PA, 1998.
[15] A.D. Becke, J. Chem. Phys. 98 (1993) 5648.
[16] C. Lee, W. Yang, R.G. Parr, Phys. Rev. B (1988) 785.
[17] M.R. Johnson, N.H. Jones, A. Geis, A.J. Horsewill, H.P. Trommsdorff, J. Chem. Phys. 116 (2002) 5694.

[18] Z. Dega-Szafran, E. Dulewicz, M. Szafran, Magn. Reson. Chem. 38 (2000) 43.

[19] Z. Dega-Szafran, M. Szafran, Bull. Acad. Pol. Sci. Chem. 43 (1995) 295.

[20] Z. Dega-Szafran, I. Kowalczyk, M. Szafran, Bull. Acad. Pol. Sci. Chem. 43 (1995) 303.

[21] J.A. Dean, Handbook of Organic Chemistry, McGraw-Hill, New York, 1987.

[22] E.P.L. Hunter, S.G. Lias, J. Phys. Chem. Ref. Data 27 (1998).

[23] G. Matsubayashi, Bull. Chem. Soc. 54 (1981) 915.

[24] H.-H. Perkampus, UV–Vis Spectroscopy and its Applications, Springer, Berlin, 1992, p. 176.

[25] A.D. Harsch, S. Johnson, D.W. Boykin, J. Chem. Soc. Chem. Commun. (1977) 119.

[26] R.A. Newmark, A. Tucker, L.C. Hardy, Magn. Reson. Chem. 34 (1996) 728.

[27] E. Pretsch, P. Buchlmann, C. Affolter, Structure Determination of Organic Compounds, Tables of Spectral Data, Springer, Berlin, 2000.

[28] C.A. Henrick, E. Ritchie, W.C. Taylor, Aust. J. Chem. 20 (1967) 2441.

[29] Z. Dega-Szafran, G. Schroeder, M. Szafran, J. Phys. Org. Chem. 12 (1999) 39.

[30] G. Schroeder, B. Łęska, A. Jarczewski, B. Nowak-Wydra, B. Brzezinski, J. Mol. Struct. 344 (1995) 77.

[31] E.D. Raczyńska, P.-C. Maria, J.-F. Gal, M. Decouzon, J. Phys. Org. Chem. 7 (1994) 725.

[32] J.W. Bunting, A. Toth, C.K.M. Hoe, R.G. Moors, J. Am. Chem. Soc. 112 (1990) 8878.

[33] K. Schwetlik, Kinettische Metoden zur Untersuchung von Reaktions Mechanism, Berlin 1971.

[34] K.A. Connors, Chemical Kinetics, The Study of Reaction Rates in Solution, VCH Publishers, New York, 1990.

[35] C. Zhu, C. Lifshitz, Chem. Phys. Lett. 320 (2000) 513.

[36] A.J. Barnes, A.C. Legon, J. Mol. Struct. 448 (1998) 101.